Article
JOURNAL OF UNIVERSITY OF BABYLON
For Pure and Applied Sciences (JUBPAS)
Vol. 33 ; No.4 | 2025

Optical Properties of (Rhodamine B with Magnetic Nano Ferrite) Preparation by PLAL for Improved Absorption Efficiency of Q-switched

Rafal A.Yass[1] , Nada S.Ahmade[2]*

[1]College of Science, University of Diyala, rafal98anbagy98@gmail.com, Diyala, Iraq
[2]College of Science, University of Diyala, nadaahmad@uodiyala.edu.iq, Diyala, Iraq..
***Corresponding author email:** nadaahmad@uodiyala.edu.iq; mobile: 07716077099

الخصائص البصرية لتحضير (رودامين B مع فيريت نانوي مغناطيسي) بواسطة PLAL لتحسين كفاءة الامتصاص لـ Q-switched

رفل عبد الحسين ياس[1], ندى سهيل احمد*[2]

1-كلية العلوم، جامعة ديالى، rafal98anbagy98@gmail.com ,ديالى, العراق

2- كلية العلوم، جامعة ديالى، nadaahmad@uodiyala.edu.iq ديالى, العراق

Accepted: 21/10/2025 **Published:** 31/12/2025

ABSTRACT

Background

Q-switching is a laser technique that temporarily stores energy in the laser medium before releasing it all at once to produce extremely brief, intense light pulses. "Q" stands for the optical cavity's quality factor, which is a gauge of how effectively it stores energy. When using Q-switching, the cavity's Q is initially kept low to avoid lasing as the population inversion increases. The stored energy can then be released in a strong pulse that is frequently nanoseconds long but has peak powers thousands of times higher than continuous wave output when the Q is abruptly switched to high.

Objective

The Co-$ZnFe_2O_4$ nanostructur is synthesis by pulsed laser ablation in liquid (PLAL) method, It is then mixed with the previously prepared Rhodamine B dye to boost optical absorption efficiency.

Materials

Uniform, surfactant-free nanoparticles are produced using a Q-switched Nd:YAG laser (1064 nm, 300 mJ). UV-Vis spectroscopy verified that the resultant nanocomposite showed increased absorption in the visible range when combined with Rhodamine B, exhibiting a discernible redshift in the absorption peak. demonstrating effective energy transfer and robust dye nanoparticle interactions.

Results

highlight the potential of Rhodamine B–Co-$ZnFeO_4$ nanostructures for high-performance uses in photocatalysis, optical sensing, and solar energy harvesting.

Conclusion

Our research shows that PLAL is a quick, easy, and efficient way to customize nanomaterials with exceptional optical qualities.

Keywords: Q-switching, Rhodamine B, PLAL.

ISSN: 2312-8135 | Print ISSN: 1992-0652
info@journalofbabylon.com | jub@itnet.uobabylon.edu.iq | www.journalofbabylon.com

ISSN: 2312-8135 | Print ISSN: 1992-0652
info@journalofbabylon.com | jub@itnet.uobabylon.edu.iq | www.journalofbabylon.com

INTRODUCTION

Nanomaterials have garnered a lot of attention because of their unique structural, magnetic, and optical properties, which make them highly helpful in advanced photonic and optoelectronic applications, Among these materials, spinel ferrites have been extensively studied due to their unique and tunable properties as saturable absorbers to improve absorption performance. In particular, cobalt zinc ferrite (CoZnFe2O4) stands out due to its saturation magnetization, large coerciveness, high coefficients of magnetostriction and good chemical stability, which make them promising candidates for saturable absorbers in passively Q-switched laser systems.

Q-switching is one of the primary methods for generating nanosecond pulses (sometimes even sub-nanosecond pulses) with solid-state lasers. The basic principle of Q-switching is that the resonator losses are kept at a high level during a pump phase, allowing one to store substantial energy in the gain medium without premature lasing, and then to suddenly switch the resonator losses to a lower value, so that a short pulse extracts a substantial fraction of the stored energy from the gain medium. Such a pulse is often called a giant (gigantic) pulse. There are two ways to control and switch intracavity losses: active and passive. While active Q-switching depends on moving or electrical parts to reduce intracavity losses and produce accurate, recurring pulses, passive Q-switching is easy to use and devoid of such components, controlling pulse emission instead using saturated absorbers (materials that change their absorption properties at high light intensities such as Co-Zn ferrte NPs) . Its simplicity makes it a preferred choice for numerous laser applications. And also inexpensive [1-5]. Laser ablation is a process in which a laser beam is used as the main instrument to ablate the target material. A laser, as a higher concentrated energy source, is centered at a specific place of the target material for the evaporation of light-absorbing materials [6].

It is widely used in prominent applications. Among its many applications are material processing (such as laser cutting and laser cleaning), medical operations like skin disease treatment, eye surgeries (like corneal correction), and tumor removal, and Synthesis of Nanoparticles involving nanoparticles of various substances, such as metals, metal oxides, and metal carbides. As it allows a controllable amount of energy in duration and dosage to be applied to the specific target area. This procedure characterized by being easy, inexpensive, quickly , and the final product's surface characteristics are readily adjustable [7, 8] . Therefore, this work aims to prepare Co–Zn

ISSN: 2312-8135 | Print ISSN: 1992-0652
info@journalofbabylon.com | jub@itnet.uobabylon.edu.iq | www.journalofbabylon.com

ferrite nanoparticles via PLAL and investigate their structural and optical properties to evaluate their potential as a saturable absorber in Q-switched laser applications.

MATERIALS AND METHODS

1- **Preparation Cobalt Zinc Ferrite nanostructure** with the general formula $Zn_xCo_{1-x}Fe_2O_4$ were synthesized by conventional chemical co-precipitation method in the Figure 1. High-purity analytical grade precursors were used, involving $Fe(NO_3)_3 \cdot 9H_2O$) ($Co(NO_3)_2 \cdot 6H_2O$),($Zn(NO_3)_2 \cdot 6H_2O$), all obtained from Sigma-Aldrich, were mixed well with (20 mL) amount of deionized water of each nitrate salt and mixed well together in glass beaker under continuous magnetic stirring at 30 C° to form a homogeneous solution. The pH of the suspension was gradually adjusted to ~12 using (15g/200ml) of sodium hydroxide (NaOH) solution, added slowly while stirring. The resulting brown precipitate was allowed to settle, and washed with deionized water and ethanol repeatedly for three times and filtered to remove unreacted ions and residual nitrate. Then, the obtained wet precipitate remained all day to dry at room temperature and its color changes from brown to black. After this, to initiate crystallization, the dried powder was subjected to heat treatment in a muffle furnace at 200 C°, to guarantee crystallization and phase formation of the spinel cobalt zinc ferrite nanoparticle

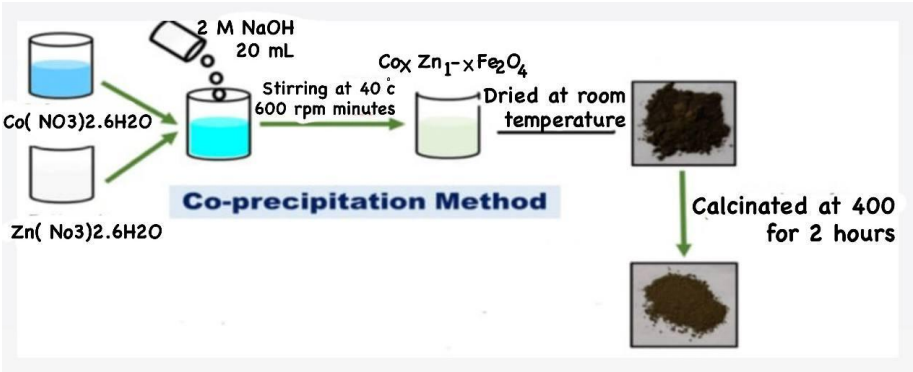

Figure (1): Chemical co-precipitation method to preparation Co-Zn ferrite.

ISSN: 2312-8135 | Print ISSN: 1992-0652
info@journalofbabylon.com | jub@itnet.uobabylon.edu.iq | www.journalofbabylon.com

2- The resulting powder was cleaned once more with distilled water and ethanol and dried for two hours at 100 ˚C . Before beginning with the PLAL process, a press powered by hydraulics was used to powder from nanostructure pellet of 10 mm diameter under a uniaxial pressure of 10 K psi.

3- **Preparation Nano particles after pillarization**, The solid metal target was immersed in a quartz cuvette containing water for laser ablation process. Pulsed laser ablation was carried out using a Q-switched Nd:YAG laser with 1064 nm, varied energy from 300 to 500 mJ . the number of pulses was 1000 for each time. The laser beam was focused onto the surface of the target as in Figure 2, with a specific duration (5-20 minutes) depending on desired concentration and size of Co-Zn ferrite NPs and the ablation was performed under magnetic stirring to ensure uniform distribution of the formed nanoparticles. Ferrite nanoparticle thin films are prepared for XRD and FESEM investigation. Finally, prepare three units of mix in nano ferrite and dye by adding 3 ml of the colloidal ferrite nanoparticles to 3 ml of rhodamine B. To analyze and determine the optical properties and bonding effect of ferrite nanoparticles, the produced samples were analyzed using a UV-Vis Spectrometer and Fourier transform infrared spectroscopy, respectively.

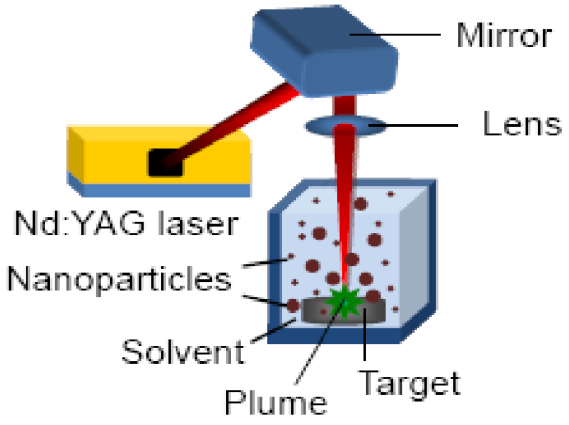

Figure (2):Preparation nano ferrite by laser ablation .

RESULTS AND DISCUSSION

The crystal structure of Co-Zn ferrite NPs prepared by the co-precipitation method is displayed in Fig. 3 by the XRD patterns. The recorded diffraction pattern confirms the formation of a single-phase spinel structure. The crystal planes (220), (311), (400), (422), (5110), and (440) are represented by the diffraction peaks that emerged at 30.1°, 35.6°, 43.1°, 53.6°, 57.1°, and 62.7°, respectively. The successful formation of the spinel phase is confirmed by that agreement with the standard data from JCPDS cards No. 22-1086 (Co ferrite) and 22-1012 (Zn ferrite). The broad peaks seen in the patterns are explained by the particles' nanoscale nature. Table 1

ISSN: 2312-8135 | Print ISSN: 1992-0652
info@journalofbabylon.com | jub@itnet.uobabylon.edu.iq | www.journalofbabylon.com

indicates that the sample's estimated particle size from the (311) plane is 17.0 nm. Because of its clarity and intensity, this peak was chosen. The prepared Co-Zn ferrite NPs are suitable for optical and magnetic applications, as demonstrated by these results, which show a highly crystalline single-phase spinel structure with nanometric size [9,10].

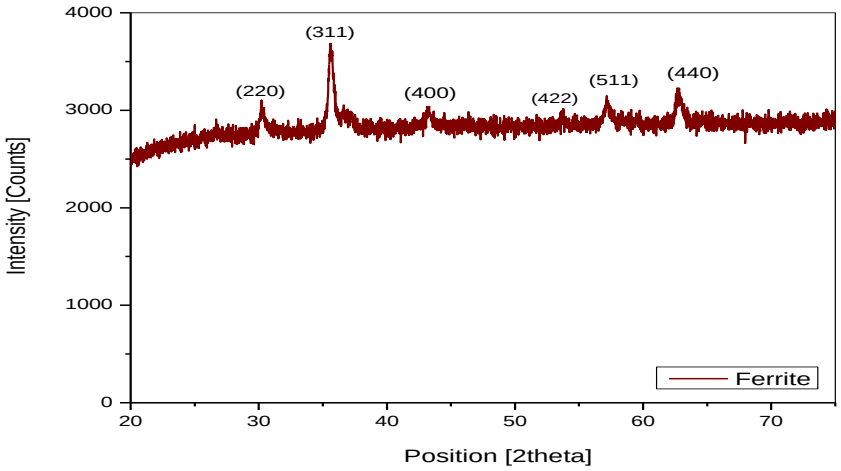

Figure 3: XRD pattern of cobalt zinc ferrite nanoparticles.

Table 1. The particle size of the sample.

NPs	Hkl	Peak position(deg.)	FWHM(deg.)	crystallite sized(nm)
Co-Zn ferrite	(220)	30.25°	0.4676	
	(311)	35.61°	0.42	17.0
	(400)	43.25°	0.5426	
	(511)	57.15°	0.4416	
	(440)	62.74°	0.4862	

3.2Field Emission Scanning Electron microscopy (FESEM):

Figure 2 illustrates the morphology and particle size of Co-Zn Fe_2O_4 NPs made by the co-precipitation method examined with a FESEM microscope. The FESEM images display the microscopic morphology and structure of ferrite nanoparticles, which are in agreement with the XRD results. The images indicate a considerable degree of ferrite particle agglomeration due to

ISSN: 2312-8135 | Print ISSN: 1992-0652
info@journalofbabylon.com | jub@itnet.uobabylon.edu.iq | www.journalofbabylon.com

its magnetic characteristics and the combination of primary particles held together by weak surface interactions such as van der Waals forces. Additionally, the nonuniform particle distribution was noted in SEM images [11,12].

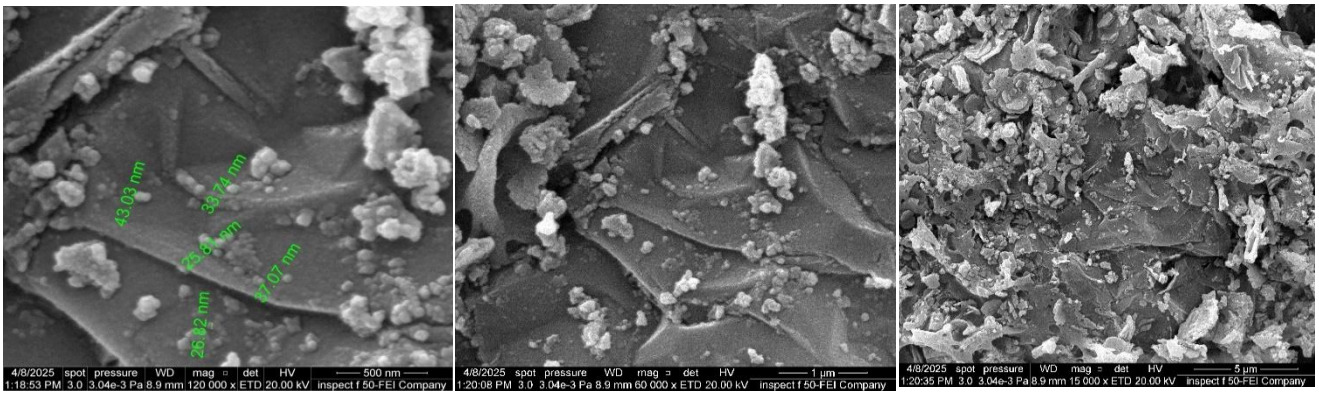

Fig 4: FESEM of Co-Zn Fe2O4 NPs prepared by laser ablation.

3.3 Ultra Violet Absorption Spectra (UV):

The optical characterization of the Rhodamine B/ferrite nanocomposites were investigated using UV–Vis absorption spectroscopy, as illustrated in **Figure 5**. The spectrum of pure Rhodamine B (Sample a) exhibits a sharp and prominent absorption peak at approximately 556 nm, which is attributed to π–π transitions in the conjugated aromatic system of the dye. Upon incorporation of cobalt–zinc ferrite nanoparticles at different concentrations (Samples b, c, and d), a gradual decrease in absorbance intensity was observed, particularly in Sample d, which contains the highest ferrite content. Furthermore, a small amount of spectral broadening was found, particularly in Sample d, which may indicate that dye–ferrite interactions have changed the dye electronic environment. These spectral changes show how increasing the ferrite content affects the system's optical response and validate that the dye and ferrite surface have successfully interacted[13-16].

ISSN: 2312-8135 | Print ISSN: 1992-0652
info@journalofbabylon.com | jub@itnet.uobabylon.edu.iq | www.journalofbabylon.com

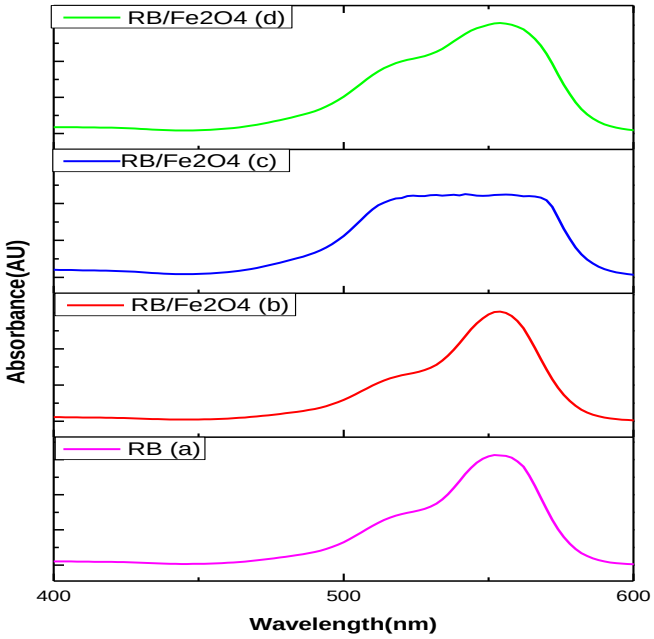

Fig 5 : Shows the UV absorption spectra of (a) Rhodamine B, (b)RB/ Ferrite 300 mJ, (c) RB/Ferrite400 mJ, (d)RB/ Ferrite 500 mJ

3.4 Fourier Transform Infrared Spectroscopy (FTIR)

The FTIR spectra was recorded in the range between 500 cm^{-1} and 4000 cm^{-1} utilizing BRUKER IFS 66 V spectrometer. The obtained FTIR spectra for both unadulterated Rhodamine b and its ferrite composite mixtures were examined to identify the vibrational changes brought on by molecular interactions, as shown in **fig 6**. the spectrum of unadulterated Rhodamine B presents several prominent absorption band located at 3430, 2920, 1586 attributed to the hydroxel stretching band, C-H band, C=C band (in the aromatic ring), respectively. And the peak observed at 1630 is consistent with[11]. After integration with Co-Zn Fe_2O_4 NPs at differ ratios (0.25,0.50, 0.75) noticeable changes were observed in the spectral features. Peak intensity around 3340 and 2920 of rhodamine b by rhodamine / Fe_2O_4 NPs modified has reduced as the ferrite ratio increases which indicate adsorption of rhodamine B onto ferrite surface, appearance of new peaks or becomes more intense especially in 1630. These spectral modification confirm that ferrite NPs influence the vibrational behavior of RB dye, likely through surface adsorption and

ISSN: 2312-8135 | Print ISSN: 1992-0652
info@journalofbabylon.com | jub@itnet.uobabylon.edu.iq | www.journalofbabylon.com

electronic interactions. In conclusion, the above results confirmed that the interaction enhancement of RB performance as saturable absorption in Q-Switching applications[17-19].

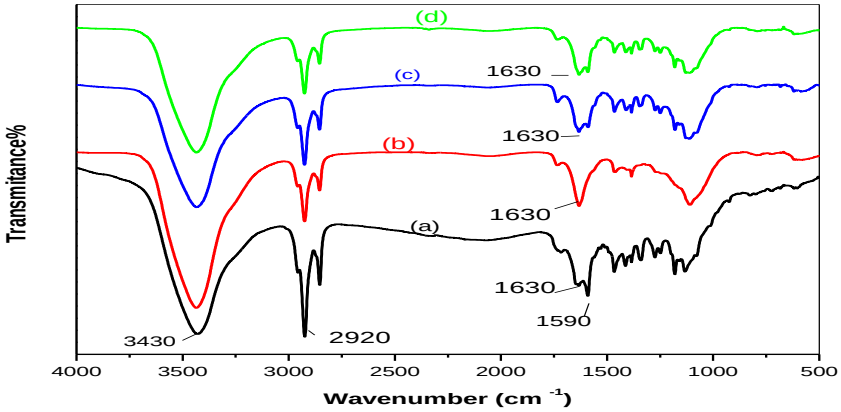

Figure 6: The FTIR spectra of (a) Rhodamine B, (b)RB/ Ferrite 300 mJ, (c) RB/Ferrite 400 mJ, (d)RB/ Ferrite 500 mJ

CONCLUSION

This study demonstrates that pulsed laser ablation in liquid (PLAL) is an efficient and environmentally friendly method for synthesizing Co-$ZnFe_2O_4$ nanoparticles and integrating them with Rhodamine B dye. The resulting nanocomposite exhibits enhanced optical absorption and redshifted absorption peaks, confirming strong interactions between the dye molecules and the ferrite nanoparticles. These findings highlight the potential of Rhodamine B–Co-$ZnFe_2O_4$ nanocomposites in optoelectronic applications, photocatalysis, and solar energy conversion. Future work can expand on this approach to develop customized nanomaterials with tunable optical properties for specific photonic and sensing technologies.

Financial support and sponsorship
Nil.

ISSN: 2312-8135 | Print ISSN: 1992-0652
info@journalofbabylon.com | jub@itnet.uobabylon.edu.iq | www.journalofbabylon.com

Conflict of interests:

There are non-conflicts of interest.

References

1. Ostendorf, A. (2021). Short Pulses. In *Handbook of Laser Technology and Applications* (pp. 247-257). CRC Press.
2. Zulkipli, N. F. (2017). *Generation of Q-Switching Pulse Train with Topology Insulators* (Master's thesis, University of Malaya (Malaysia)).
3. Zhu, K., Ju, Y., Xu, J., Yang, Z., Gao, S., & Hou, Y. (2018). Magnetic nanomaterials: Chemical design, synthesis, and potential applications. *Accounts of chemical research*, *51*(2), 404-413.
4. Vinosha, P. A., Manikandan, A., Ceicilia, A. S. J., Dinesh, A., Nirmala, G. F., Preetha, A. C., ... & Xavier, B. (2021). Review on recent advances of zinc substituted cobalt ferrite nanoparticles: Synthesis characterization and diverse applications. *Ceramics International*, *47*(8), 10512-10535.
5. Hou, Y., & Sellmyer, D. J. (Eds.). (2017). *Magnetic nanomaterials: Fundamentals, synthesis and applications*. John Wiley & Sons.
6. Shahid, M., Sagadevan, S., Ahmed, W., Zhan, Y., & Opaprakasit, P. (2022). Metal oxides for optoelectronic and photonic applications: A general introduction. In *Metal Oxides for Optoelectronics and Optics-Based Medical Applications* (pp. 3-31). Elsevier.
7. Saha, A., Bhattacharjee, L., & Bhattacharjee, R. R. (2023). Synthesis of carbon quantum dots. In *Carbon Quantum Dots for Sustainable Energy and Optoelectronics* (pp. 39-54). Woodhead Publishing.
8. Torrisi, L., & Torrisi, A. (2018). Laser ablation parameters influencing gold nanoparticle synthesis in water. *Radiation Effects and Defects in solids*, *173*(9-10), 729-739.
9. Narsimulu, D., Padmaraj, O., Srinadhu, E. S., & Satyanarayana, N. (2017). Synthesis, characterization and electrical properties of mesoporous nanocrystalline CoFe 2 O 4 as a negative electrode material for lithium battery applications. *Journal of Materials Science: Materials in Electronics*, *28*, 17208-17214.
10. Naskar, A., Khan, H., & Jana, S. (2017). Protein adsorption capability of zinc ferrite nanoparticles formed by a low-temperature solution-based process. *Research on Chemical Intermediates*, *43*, 7041-7053.
11. Li, Y. L., Wang, W. X., Wang, Y., Zhang, W. B., Gong, H. M., & Liu, M. X. (2018, May). Synthesis and Characterization of rhodamine B-ethylenediamine-hyaluronan acid as potential biological functional materials. In *IOP Conference Series: Materials Science and Engineering* (Vol. 359, No. 1, p. 012040). IOP Publishing.
12. Marwa Hazem Sabbar, Improving the properties of magnetic nano particles (Co_Ni) ferrite by pulsed laser deposition and studying its biological effect,(2022), Diyala Journal of Pure Sciences.

13. Tatarchuk, T. R., Bououdina, M., Paliychuk, N. D., Yaremiy, I. P., & Moklyak, V. V. (2017). Structural characterization and antistructure modeling of cobalt-substituted zinc ferrites. *Journal of Alloys and Compounds*, *694*, 777-791.

14. Tatarchuk, T. R., Paliychuk, N. D., Bououdina, M., Al-Najar, B., Pacia, M., Macyk, W., & Shyichuk, A. (2018). Effect of cobalt substitution on structural, elastic, magnetic and optical properties of zinc ferrite nanoparticles. *Journal of Alloys and Compounds*, *731*, 1256-1266

15. Andhare, D. D., Patade, S. R., Kounsalye, J. S., & Jadhav, K. M. (2020). Effect of Zn doping on structural, magnetic and optical properties of cobalt ferrite nanoparticles synthesized via. Co-precipitation method. *Physica B: Condensed Matter*, *583*, 412051.

16. Andhare, D. D., Patade, S. R., Jadhav, S. A., Somvanshi, S. B., & Jadhav, K. M. (2021). Rietveld refined structural, morphological, Raman and magnetic investigations of superparamagnetic Zn–Co nanospinel ferrites prepared by cost-effective co-precipitation route. *Applied Physics A*, *127*(6), 480.

17. Darwish, M. S. (2023). Magnetite@ zinc cobalt ferrite nanoparticles: synthesis, magnetic behavior, and optical properties. *Crystals*, *13*(8), 1284.

18. Shaker, D. M., Ahmed, R. R., Mohammad, A. M., Mubarak, T. H., & Mohamed, I. H. (2024). Synthesis and Characterization of CoZnFe2O4 Ferrite Nanoparticles by Co-precipitation Method for Biomedical Applications. *Passer Journal of Basic and Applied Sciences*, *6*(2), 488-

19. Kumar, A. (2025). Structural, magnetic and dielectric properties of MWCNTs-incorporated Cobalt-Zinc Ferrite Nanocomposites. *Ceramics International*.

20. Hakem, A. A. L., & Ali, A. D. G. (2016). Morphology and Optical properties of (Fe-Cd) core-shell by Laser Ablation in Ethanol. *International Journal of ChemTech Research*, *9*(10), 131-138.

ISSN: 2312-8135 | Print ISSN: 1992-0652
info@journalofbabylon.com | jub@itnet.uobabylon.edu.iq | www.journalofbabylon.com

ISSN: 2312-8135 | Print ISSN: 1992-0652
info@journalofbabylon.com | jub@itnet.uobabylon.edu.iq | www.journalofbabylon.com

الخلاصة

المقدمة

تبديل Q هو تقنية ليزر تُخزّن الطاقة مؤقتًا في وسط الليزر قبل إطلاقها دفعةً واحدةً لإنتاج نبضات ضوئية شديدة وقصيرة للغاية. يرمز "Q" إلى معامل جودة التجويف البصري، وهو مقياس لمدى فعالية تخزين الطاقة. عند استخدام تبديل Q، يُحافظ على معامل جودة التجويف في البداية منخفضًا لتجنب إصدار أشعة الليزر مع ازدياد انعكاس السكان. ثم يُمكن إطلاق الطاقة المخزنة في نبضة قوية، غالبًا ما تكون مدتها نانوثانية، لكن طاقاتها القصوى أعلى بآلاف المرات من طاقة الموجة المستمرة عند تحويل معامل الجودة فجأةً إلى مستوى عالٍ.

الهدف

يتم تصنيع البنية النانوية لـ $Co–ZnFe_2O_4$ بطريقة الاستئصال بالليزر النبضي في السائل (PLAL)، ثم يتم خلطها مع صبغة Rhodamine B المعدة مسبقًا لتعزيز كفاءة الامتصاص البصري.

طرق العمل

تم إنتاج جسيمات نانوية متجانسة وخالية من المواد الخافضة للتوتر السطحي باستخدام ليزر Nd:YAG متحول Q–switched (1064 نانومتر، 300 ميلي جول). وقد أثبت التحليل الطيفي للأشعة فوق البنفسجية والمرئية أن المركب النانوي الناتج أظهر امتصاصًا متزايدًا في النطاق المرئي عند دمجه مع رودامين ب، مما أظهر انزياحًا أحمر واضحًا في ذروة الامتصاص. مما يُظهر نقلًا فعالًا للطاقة وتفاعلات قوية بين جسيمات الصبغ النانوية.

النتائج

تسلط الضوء على إمكانات هياكل النانو Rhodamine B–$Co–ZnFeO_4$ للاستخدامات عالية الأداء في التحفيز الضوئي والاستشعار البصري وتجميع الطاقة الشمسية.

الاستنتاج

تظهر أبحاثنا أن PLAL هي طريقة سريعة وسهلة وفعالة لتخصيص المواد النانوية بخصائص بصرية استثنائية.